AIAA JOURNAL
Vol. 44, No. 6, June 2006

Optimization of Controlled Jets in Crossflow

S. R. Shapiro,* J. M. King,† R. T. M'Closkey,‡ and A. R. Karagozian§
University of California, Los Angeles, Los Angeles, California 90095-1597

The controlled acoustical excitation of a round gas jet injected transversely into crossflow, is studied. Use of an open-loop, or feedforward, controller in the experiments allowed for straightforward comparisons to be made among jet responses to different conditions of acoustic excitation of jet fluid. It was found that, for a variety of excitation frequencies, optimal temporal pulse widths during square wave excitation produced clear and distinctly rolled-up vortical structures as well as increased jet penetration into the crossflow for jet-to-crossflow velocity ratios of 2.6 and 4.0. In some cases, application of forcing frequencies corresponding to subharmonics of the upstream shear layer mode for the unforced transverse jet also produced increased jet penetration, coincident with deeply penetrating, distinct vortical structures in the jet. In other instances, merely exciting at the optimal pulse width and at a low excitation frequency (in comparison to the unforced transverse jet shear layer frequency) yielded the best jet penetration and spread. These results on optimization may be interpreted in terms of a universal timescale associated with vortex ring formation and propagation.

Introduction

TRANSVERSE jets, or jets injected normally into crossflow, have been studied extensively[1–6] because of their widespread applications, particularly in aerospace propulsion devices. One significant observation in transverse jet experiments has been that of the dominance of a counter-rotating vortex pair associated with the jet cross section, particularly in the far field,[3] but with evidence of its initiation in the near field of the jet.[4–6] Mean measurements of the flowfield suggest that improved mixing in the transverse jet (over that of a jet injected into a quiescent fluid) may be due to enhanced entrainment of the crossflow into the injected fluid, resulting, at least in part, from the development and actions of the counter-rotating vortex pair.

Through temporal excitation of the transverse jet fluid, active control of vorticity generation and hence, potentially, injectant mixing processes may be accomplished. Recent experiments on pulsed or acoustically excited transverse jets[4,7,8–12] suggest that, for certain excitation conditions, increased jet penetration into the crossflow and/or increased mixing may be achieved. Yet, specific conditions yielding increased penetration vary rather widely among these different sets of experiments, which have been conducted in both liquids[9,10] and gases.[4,7,8,11,12] Some of these studies have focused on sinusoidal excitation[4,8,12] and find improvement in transverse jet mixing at specific values of the Strouhal number (based on mean jet velocity and jet orifice diameter, $Sr_j \equiv f D_j/\bar{U}_j$). In some cases, for example, in the gas-phase experiments by Narayanan et al.,[12] the forcing frequency for maximized jet spread and mixing is equal to or greater than that associated with the unforced transverse jet's shear layer; in these experiments, the mean jet-to-crossflow velocity ratio $R \equiv \bar{U}_j/U_\infty = 6$. In other cases, for example, in the gas-phase experiments by M'Closkey et al.,[7] there is little response of the jet, even to high-amplitude sinusoidal excitation, irrespective of the applied frequency. Yet, these experiments are for a lower value of R, namely, 2.58.

Still other studies[7,9–11] utilize square wave excitation for the transverse jet, with the ability to modify both excitation frequency f and the duty cycle α of the waveform, the latter of which is defined as the ratio of the temporal pulse width τ to the period T of square wave excitation, where $T \equiv 1/f$. Studies of fully modulated transverse jets by Johari et al.,[9] for example, suggest that optimal jet penetration and spread may occur for specific values of the Strouhal number and relatively low values of duty cycle, on the order of $\alpha = 20\%$. More recent scaling analysis by Johari[13] proposes a classification scheme for the pulsed jet in crossflow that explores the influences of the square wave's stroke ratio (related to forcing amplitude) and duty cycle. Penetration and mixing are observed to be strongly dependent on the degree of interaction among flow structures near the jet nozzle and in the far field.

In prior gas-phase transverse jet experiments by our group,[7] a dynamic compensator or feedforward controller is developed and utilized to be able to generate more accurately temporal waveforms at the jet exit plane. The compensator enables the detailed examination of the excitation conditions (for square wave excitation, the forcing frequency f, duty cycle α, and/or pulse width τ) that lead to improved jet penetration via the generation of distinct, deeply penetrating vortical structures. For the single jet-to-crossflow velocity ratio examined in these studies, $R \equiv \bar{U}_j/U_\infty = 2.58$, optimal jet penetration and spread conditions are found to occur for square wave excitation at subharmonics of the natural (unforced) upstream shear layer mode f_n of the transverse jet, with specific pulse widths of the order $\tau \approx 3$ ms. At higher forcing frequencies (especially those well above the first subharmonic, $f_n/2$), transverse jet response is not much different from that of the unforced jet in crossflow, even at high amplitudes of forcing. Moreover, as noted earlier, sinusoidal forcing at any frequency, even with amplitudes exceeding 75% of the mean jet velocity, do not appear to alter transverse jet behavior substantially in this range of low R values. These observations differ from those of Narayanan, et al.,[12] who, in gas-phase experiments of the pulsed transverse jet, observe significant enhancements in jet mixing, by about 30–40%, yet with only marginal increases in penetration. However as noted earlier, these experiments[12] pertain to a value of $R = 6$.

The present experimental study seeks to continue an examination of the optimization of the acoustically excited jet in crossflow. The dynamic compensator allows relatively accurate generation of desired temporal waveforms to be produced at the jet exit plane and, hence, provides the ability to systematically study conditions that could increase transverse jet penetration and spread and the relation

Presented as Paper 2003-0634 at the AIAA 41st Aerospace Sciences Meeting, Reno, NV, 6–9 January 2003; received 12 August 2005; revision received 18 November 2005; accepted for publication 29 November 2005.

*Graduate Researcher, Department of Mechanical and Aerospace Engineering; currently Film Editor, Truepictures Productions.

†Graduate Researcher, Department of Mechanical and Aerospace Engineering; currently at Advance Air Vehicle Design Department, Northrop–Grumman Corporation, El Segundo, CA 90245-2804.

‡Associate Professor, Department of Mechanical and Aerospace Engineering.

§Professor, Department of Mechanical and Aerospace Engineering, 46-147 K Engineering IV; ark@seas.ucla.edu. Fellow AIAA.

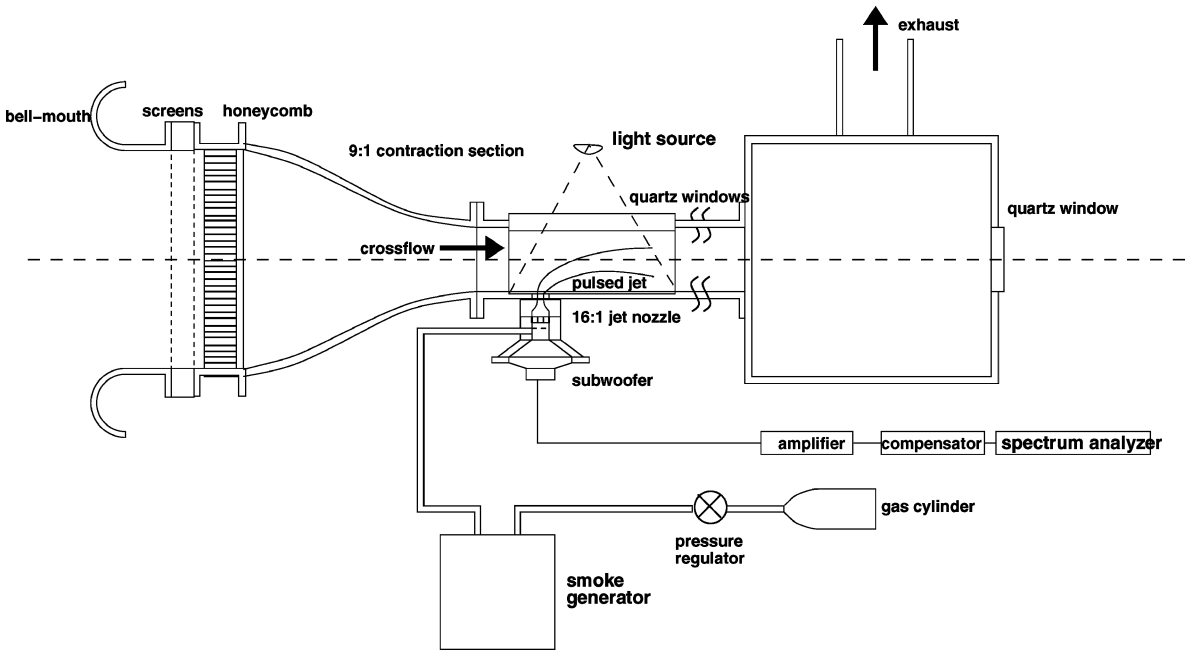

Fig. 1 Experimental setup for acoustically controlled jet in crossflow.

of these conditions to the control of vorticity generation at the jet exit plane.

Experimental Facility and Methods

The present experimental configuration, shown in Fig. 1, utilized a wind tunnel that created crossflow velocities U_∞ in the range from 1.1 to 10.0 m/s. The tunnel had a 12×12 cm test section consisting of a steel-plated bottom with interchangeable walls of ceramic or quartz windows. There were three additional tunnel sections actually present downstream of that shown in Fig. 1. The jet orifice was located 9.51 cm downstream of the end of the tunnel contraction section. The mean jet exit velocity $\bar{U}_j$ ranged from 1.1 to 9.7 m/s, and the jet orifice inner diameter D_j was fixed in these studies at 7.62 mm. The jet was formed by a 16:1 contraction ratio nozzle, designed using a fifth-order polynomial shape, connected to a circular cylinder with a length of 14 cm. Upstream of the circular cylinder was a small plenum in which a loudspeaker used for acoustical excitation of the jet was mounted. The jet fluid, gaseous nitrogen, was injected into the circular cylinder from a compressed gas cylinder, and its mean flow rate was measured using a Tylan mass flowmeter. For the conditions explored in the present studies, the wall boundary layer was approximately one jet diameter in thickness just upstream of the jet orifice.

For this experiment, a single component hot-wire anemometer calibrated by a pitot probe was used to measure the temporally evolving velocities at the jet exit plane. Uncertainties in the velocity were approximately 3%, but they were higher at lower velocities, those approaching 1 m/s. For these temporally evolving velocity measurements, the hot wire was placed at the center of the jet nozzle exit, nearly coincident with the injection wall. The dominant jet instabilities in the upstream shear layer of the unforced jet in crossflow were quantified by placing the hot wire within 1 to 1.5 diameters above the jet exit, along its trajectory, with a signal analyzer acquiring power spectra in the range 40–1600 Hz. Instabilities at the edge of the transverse jet shear layer are generally thought to be of the Kelvin–Helmholtz type (see Refs. 2, 4, 14, and 15). Ongoing studies[16–18] are exploring the nature of these instabilities. In the present experiments, the hot-wire position for the spectra was varied within the upstream jet shear layer until clearly resolved peaks, representing fundamental shear layer mode frequencies f_n and their higher harmonics, were obtained, indicating the initiation of nonlinear shear layer behavior.

Smoke visualization was used to observe jet behavior. Quartz windows adjacent to the jet injection region and a 500-W light source above the test section allowed this visualization, shown in Fig. 1. A heated seeder using a liquid parafin solution was used for smoke generation. The nitrogen injectant passed through the seeder, then through an ice bath that allowed the injectant to enter the wind tunnel at temperatures that were verified to be equal to that of the crossflow.[19] To aid in the visualization of the jet, the walls of the tunnel were sooted for increased resolution. During smoke visualization, a camera [in earlier experiments, a Nikon N2000 SLR and later a Nikon D100 charge-coupled device camera] was positioned in front of the test section of the tunnel. The visualizations of the transverse jet were recorded with long (1/15 s) and short (1/2000 s) exposures.

The loudspeaker for the acoustically excited jet was driven by a function generator and amplifier, with feedforward control by the dynamic compensator, used to form the desired square or square-like waveforms at the jet exit. An overview of the compensator is provided in the next section.

Feedforward Controller or Compensator

As described in detail by M'Closkey et al.,[7] the jet actuation system is composed of the amplifier, loudspeaker, jet plenum, and nozzle. The actuator is such that its dynamics alter the desired temporal input waveform introduced by the signal generator, so that the output waveform measured at the jet exit by the hot wire is distorted. This distortion is significant in the case of square wave excitation, but only minor in the case of sinusoidal excitation. The frequency dependence of the amplitude and phase of the output signal requires development and implementation of a dynamic compensator, or feedforward controller. The compensator is developed via a mathematical inversion of a linear model representing the frequency response for the jet actuation system. This frequency response is dependent in general on the specific jet and crossflow conditions. When the inversion, or compensator, is applied to the forced jet, there results a much flatter frequency response for the actuator. As a result, there is a more precisely prescribed temporally varying jet exit velocity. With imposition of the feedforward control to create a more nearly square wave excitation of the jet, specific parameters can be made nearly equal among different excitation conditions, for example, the rms amplitude of velocity excitation and/or the temporal pulsewidth of the excitation.

As detailed by M'Closkey et al.,[7] the compensator is seen to have a significant effect on square waveform excitation of the jet. The compensator forces the waveform to resemble more closely a square wave with essentially the desired duty cycle. Higher-frequency

ringing in the waveform does occur in specific excitation cases, as will be shown for the present studies. Although the elimination of this ringing is the subject of ongoing studies,[20,21] as long as the temporal waveform has a sharp upsweep for the delivery of sharp pulses of vorticity, and a relatively sharp downsweep to more clearly define the pulsewidth, the ringing appears to have very little effect on transverse jet behavior.

Smoke visualization[7] reveals that, with a better delineated square wave due to compensation, deeply penetrating and rather distinct vortex rings can be introduced into the flowfield at the frequency of excitation, resulting under certain circumstances in significant increases in jet penetration and spread. The offline control allowed by the dynamic compensator thus permits a comparison of the effects of different excitation frequencies and duty cycles on jet behavior, which is the main focus of the present study.

Results

The present experiments considered the optimization of four distinct cases for the jet in crossflow. The four cases, numbered 1–4 and defined by their spatially averaged jet velocity $\bar{U}_j$ and crossflow velocity U_∞, are shown Table 1. Also shown in Table 1 are other parameters to be discussed in detail hereafter. The four cases corresponded to two distinct jet-to-crossflow velocity ratios R and four different jet velocities (and, hence, four different jet Reynolds numbers $Re_j \equiv \bar{U}_j D_j/\nu$). Spatial profiles of the velocity at the nozzle exit were generally flat, although at the lower jet-to-crossflow velocity ratio, $R = 2.58$, deflection of the jet by the crossflow was observed at the upstream edge of the jet. For most cases described, the momentum thickness of the jet boundary layer was of the order of $0.05 D_j$.

To characterize accurately the behavior of the jet in crossflow, the dominant upstream shear layer frequencies for the unforced transverse jet f_n were quantified from power spectra measured by the hot wire. Plots of two of the four cases' power spectra, for example, are shown in Figs. 2a and 2b. The distinct peaks and higher harmonics in the power spectra occurred when the hot wire was placed in the region observed (in separate smoke images) to contain rolled-up near-field vortices. Clearly delineated higher harmonics of the dominant shear layer frequency were also observed, indicating the initiation of nonlinear behavior in the instability. These higher harmonics were observed for all cases explored in the present studies. The measured values of f_n and associated Strouhal numbers Sr_j for each case explored are shown in Table 1.

When the compensator was used, the effect of square wave excitation on jet behavior was examined in detail. Sine wave excitation was observed in prior experiments[7] not to have a significant effect in increasing jet penetration and spread, for jet and crossflow conditions similar to case 1 in Table 1, even with very large-amplitude excitation. Hence, the present experiments, with a maximum R of 4, focused only on square wave excitation. Separate experiments exploring the tranverse jet's shear layer instabilities,[16,17] for a wide range of R values, suggest that sinusoidal forcing for relatively low values of R (below about six) may have little influence on jet response because the jet's shear layer may undergo by a different type of instability than that which exists at higher R values. This issue continues to be explored separately; in the present sets of experiments, however, only square wave excitation was employed for values of $R = 2.58$ and 4.0.

In the present tests, $U'_{j,\mathrm{rms}}$ was matched for each case in Table 1 for a wide variety of excitation frequencies and duty cycles α (or temporal pulse widths τ). This matching effectively delivered a scaled excitation impulse to the jet fluid (impulse being proportional to the square of the average excitation velocity) among different forcing conditions. A critical or minimum excitation level $U'_{j,\mathrm{rms}}$ was required for the jet to respond in any significant way to the excitation. The matched $U'_{j,\mathrm{rms}}$ value was always chosen to lie above this critical level to compare adequately the effects of different frequencies, duty cycles, and, hence, pulse widths of acoustical excitation on transverse jet behavior. Yet in all cases the excitation velocities were chosen to be small enough so that the jets were never fully modulated, and, hence, the velocity at the jet exit never became negative. The chosen values of $U'_{j,\mathrm{rms}}$ for each set of excitation experiments are listed in Table 1.

Table 1 Operating conditions for present jet in crossflow experiments, measured dominant near-field shear layer frequencies f_n, and associated Strouhal numbers for unforced transverse jet

Case	$\bar{U}_j$, m/s	U_∞, m/s	R	Re_j	$U'_{j,\mathrm{rms}}$, m/s	f_n, Hz	Sr_j
1	2.8	1.1	2.58	1420	1.5	220	0.60
2	4.3	1.1	4.0	2200	1.8	454	0.80
3	5.6	2.2	2.58	2830	2.2	600	0.82
4	7.2	1.8	4.0	3660	2.3	870	0.92

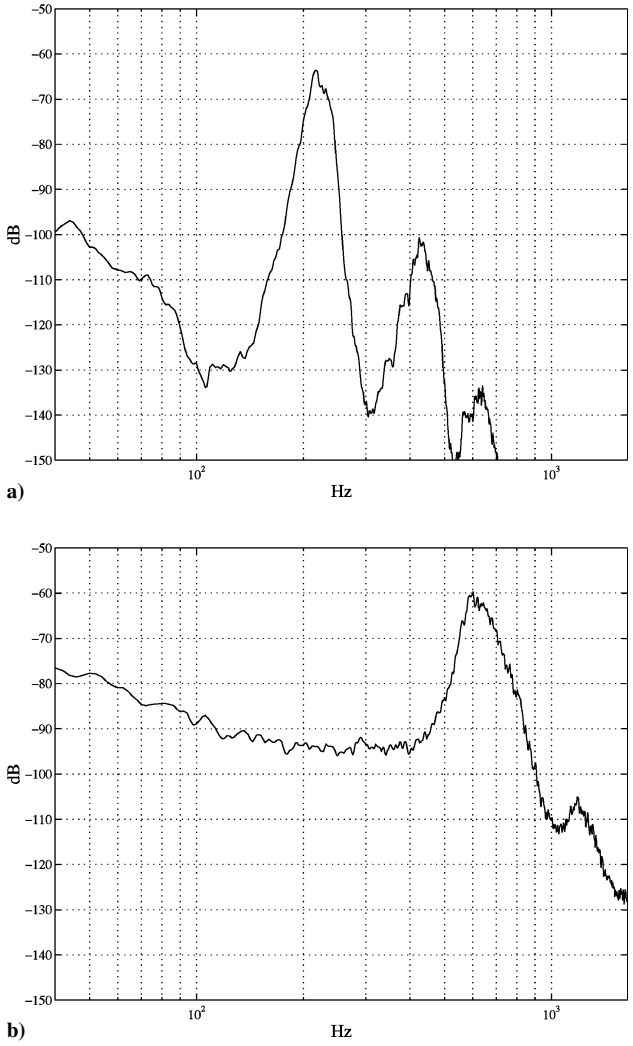

Fig. 2 Power spectra (amplitude of hot-wire voltage, measured in decibels, as function of frequency) for experimental cases 1 (shown in panel a) and 3 (shown in panel b) in the absence of acoustic excitation. Natural shear layer instabilities and higher harmonics are revealed.

In Fig. 3, sample waveforms for selected excitation cases of the transverse jet show the desired input waveforms from the function generator and the compensated temporal waveform at the center of the jet exit orifice measured by the hot-wire anemometer. Each waveform shown has the mean subtracted. For each experimental case, two plots are shown in each of Figs. 3a-3d to show the matching of the rms of the velocity excitation $U'_{j,\mathrm{rms}}$ and the average pulse width τ for two different forcing frequencies f and duty cycles α. For example, the solid waveforms shown in Fig. 3b display two different excitation conditions for case 2 (where $\bar{U}_j = 4.3$ m/s and $U_\infty = 1.1$ m/s). The plot on the left has an input square wave frequency of 151.3 Hz and pulse width of 2.3 ms, and the plot on the right has $f = 113.5$ Hz and $\tau = 2.3$ ms, whereas the value of $U'_{j,\mathrm{rms}}$ was matched at 1.8 m/s for each condition by adjusting the

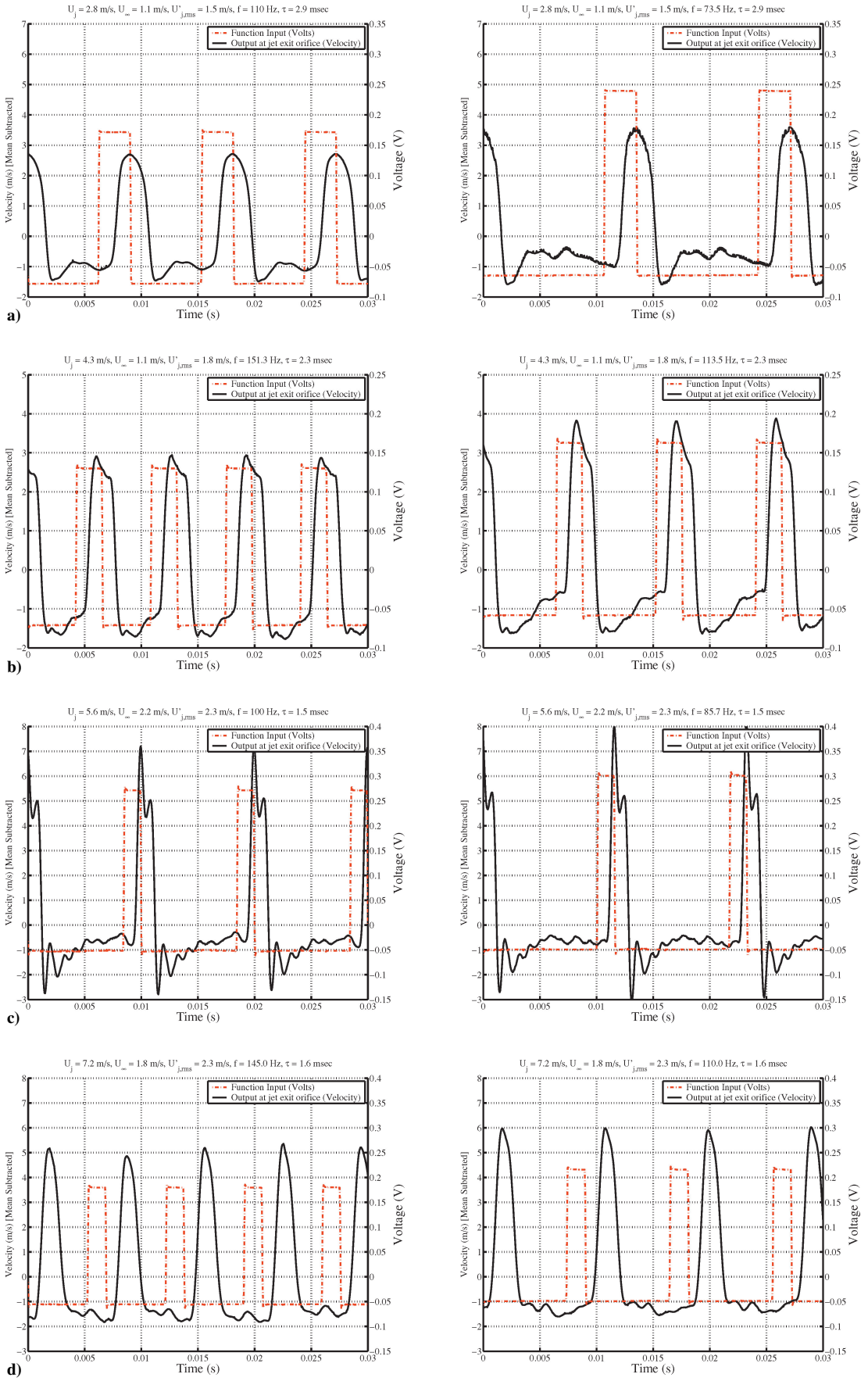

Fig. 3 Compensated temporal velocity waveforms, with mean subtracted, measured at the center of the jet exit plane (solid line) for the four different experimental cases, compared with input waveforms (dashed line). "Matched" $U'_{j,rms}$ values (indicated in Table 1) and closely matched pulse widths τ were used for each set of waveforms: a) case 1; left: f = 110 Hz, τ = 2.9 ms; right: f = 73.5 Hz, τ = 2.9 ms; b) case 2; left: f = 151.3 Hz, τ = 2.3 ms; right: f = 113.5 Hz, τ = 2.3 ms; c) case 3; left: f = 100 Hz, τ = 1.5 ms; right: f = 85.7 Hz, τ = 1.5 ms; and d) case 4; left: f = 145 Hz, τ = 1.6 ms; right: f = 110 Hz, τ = 1.6 ms.

amplitude of forcing. By studying the jet response to these and many other conditions, one could then determine which specific excitation conditions resulted in improved jet penetration and spread and/or in the periodic formation of distinct vortical structures.

Smoke visualization for all of the four experimental cases yielded very consistent results. One notable observation was that specific values of the temporal pulse width τ, for a variety of different forcing frequencies, resulted in the generation of distinct, deeply penetrating vortical structures. For example, Fig. 4 shows that, for case 1 with square wave excitation at a fixed frequency f, when the duty cycle α (or pulse width $\tau = \alpha/f$) was increased, the jet penetration reached a maximum at a specific value of α and then decreased for higher values of α. This maximum in the penetration appeared to occur under conditions where the jet formed the most distinct vortical structures at the nozzle exit plane. In Fig. 4, these conditions correspond to $\alpha = 30\%$ or $\tau \cong 3$ ms. This same value of τ produced the deepest penetrating, most distinct vortical structures at other forcing frequencies for case 1. Note, however, that although the production of deeply penetrating vortical structures was achieved at these rather specific values of excitation pulse width τ, these conditions often produced strongly bifurcated jets, as shown in the long exposure images in Fig. 4. Hence, optimal vortex ring penetration, in general, may not necessarily produce optimal injectant mixing with crossflow.

The preceding observation was made for every experimental set of conditions examined here. In fact, for each experimental condition examined (cases 1–4 in Table 1), there was, in general, only one value of τ that resulted in the greatest jet penetration for matched $U'_{j,\mathrm{rms}}$ values and for a variety of forcing frequencies. These values of τ_{opt} producing optimal vortex ring penetration are given in Table 2.

The appearance of specific values of an optimal pulse width τ_{opt} occurred in many cases for acoustical forcing at both subharmonic and nonsubharmonic frequencies of the natural vortex roll-up mode. For certain experimental conditions with low R and Re_D values, for example, case 1, the maximum jet penetration occurred for cases where τ_{opt} was employed and, in addition, a subharmonic forcing frequency of the natural shear layer mode was applied. In Fig. 5a, for example, smoke images for case 1 indicate that when the pulse width was fixed at approximately $\tau_{\mathrm{opt}} \cong 3$ ms, the deepest penetration and most distinct vortical structures occurred when the applied frequency corresponded to a subharmonic of $f_n = 220$ Hz, that is, 44, 55, 73.5, and 110 Hz. At other nonsubharmonic frequencies, for example, 85 and 125 Hz, fairly distinct vortical structures were formed, but they and the jet, in general, did not penetrate into the crossflow as well as for subharmonic forcing. For relatively high forcing frequencies, well above $f_n/2$, for example, 147 Hz as shown, there was little response of the jet to forcing, despite that the rms of the velocity excitation $U'_{j,\mathrm{rms}}$ was matched at these values for all images in Fig. 5a.

When the R value was increased to 4.0 and the shear layer frequency was relatively high, for example, $f_n = 870$ Hz for experimental case 4, both subharmonic and nonsubharmonic forcing produced good penetration of the jet and vortical structures. In Fig. 5b,

Table 2 Values of pulse width $\tau = \tau_{\mathrm{opt}}$ that maximized jet penetration and vortex ring formation and penetration for different experimental cases studied

Case	τ_{opt}, ms
1	3.0
2	2.5
3	1.7
4	1.6

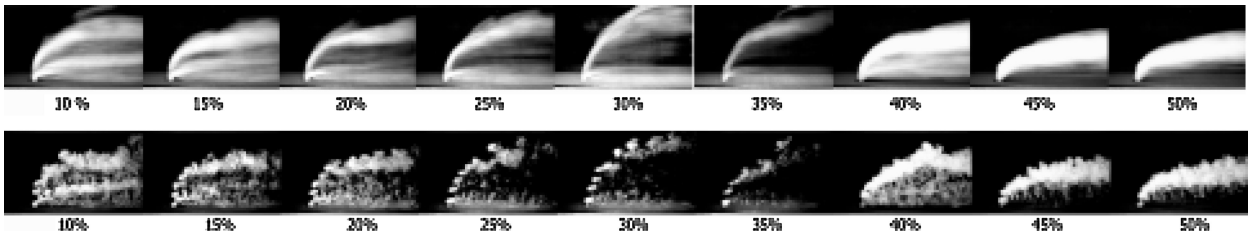

Fig. 4 Smoke visualization for experimental case 1 with forcing frequency f = 110 Hz and for duty cycles α ranging from 10 to 50%. Upper images display long exposure photographs and lower images display short exposure photographs. Maximum jet penetration was observed to occur at duty cycle of about 30%, corresponding to temporal pulse width of τ = 3 ms.

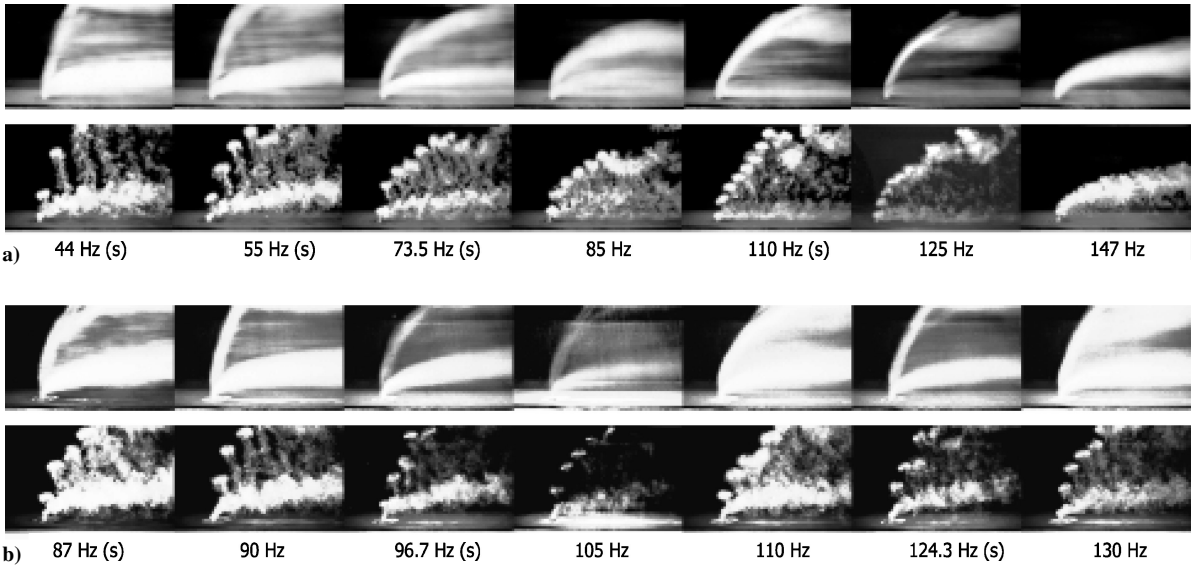

Fig. 5 a) Experimental case 1, with fixed input pulse width τ_{opt} = 3.0 ms and jet perturbation level $U'_{j,\mathrm{rms}}$ = 1.5 m/s, for forcing frequency f swept between 44 and 147 Hz. b) Experimental case 4, with fixed input pulse width τ_{opt} = 1.6 ms and jet perturbation level $U'_{j,\mathrm{rms}}$ = 2.3 m/s, for forcing frequency swept between 87 and 130 Hz; subharmonic forcing is denoted by (s).

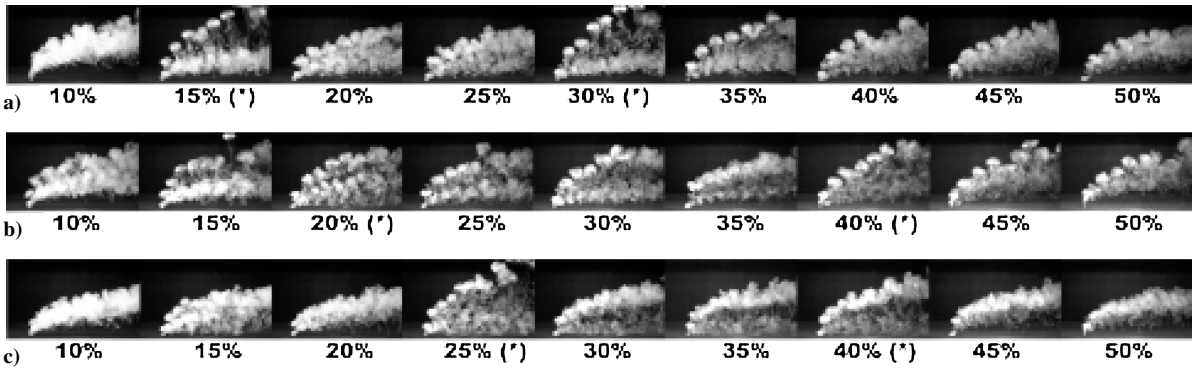

Fig. 6 Smoke visualization at short exposure times for acoustically forced transverse jets, for experimental case 1, with peak-to-peak ΔU_j fixed at 4.8 m/s; results are shown for forcing frequencies of a) 55, b) 73.5, and c) 85 Hz, with sweep in duty cycle α from 10 to 50%, where $*$ refers to conditions producing maximum jet penetration.

for example, as long as the pulse width was matched at $\tau_{\text{opt}} \cong 1.6$ ms, subharmonic as well as nonsubharmonic forcing frequencies produced uniformly good jet response. Yet, the excitation conditions producing these deeply penetrating jets always required very low forcing frequencies, that is, those well below one-half of the shear layer mode, consistent with the observations by Johari et al.,[9] in liquids. Furthermore, in Fig. 5b, one finds that because different frequencies with a fixed pulse width could produce deep jet penetration, one can optimize penetration with different values of duty cycle α and, thus, different distributions of high- and low-momentum fluid. Hence, in the sweep of frequencies shown in Fig. 5b, one can have very different levels of mixing and injectant distribution, despite very similar jet penetration and overall spread. Note, however, that the independence of frequency exhibited in Fig. 5b may have resulted from simply applying a sufficiently large jet excitation velocity $U'_{j,\text{rms}}$. Large enough excitations to the jet fluid could have caused the input forcing frequency to dominate in the influence of jet behavior, rather than that of a subharmonic frequency via multiple vortex merging.[22] This issue is being explored in ongoing experiments.

To further examine the issue of optimizing jet penetration via distinct vortex formation, the concept of the universal timescale associated with coherent vortex ring formation, proposed by Gharib et al.,[23] was explored. These researchers find that a piston-generated vortex ring attains a maximum circulation and is disconnected from its trailing jet at critical values of the ratio of piston stroke length L to diameter D, corresponding to a "universal time scale of vortex formation." These critical values for distinct vortex ring formation and propagation appear in the range $3.6 \leq L/D \leq 4.5$. Whereas the present experiments involved the acoustically pulsed continuous jet, rather than piston-driven starting vortex rings, the observation of a critical timescale for distinct ring formation, τ_{opt}, suggests a similar physical mechanism for enhanced penetration.

One may consider an analog to the stroke length L (for piston-generated vortex rings) in the present experiments to be the product of the peak-to-peak velocity excitation amplitude ΔU_j and the pulse width τ. The vortex tube diameter D may be considered to be equivalent to the transverse jet diameter D_j. Thus, to examine the concept of the optimal L/D ratio, the present experiments had to be conducted by matching ΔU_j among different excitation conditions and observing if there were critical values of τ that created optimal vortex formation and deeply penetrating jets. Figure 6 shows, for experimental case 1 and for three different forcing frequencies with matched values of the peak-to-peak velocity amplitude ΔU_j, smoke images where the duty cycle α (and, hence, pulse width τ) was swept from low to high values. Interestingly, for each forcing frequency, there were two distinct values of pulse width that produced the deepest penetrating jets. At 55 Hz, for example (Fig. 6a), as duty cycle was increased from 10%, the jet and vortex ring penetration reached a peak at $\alpha = 15\%$ (or $\tau \cong 2.7$ ms), then decreased, then increased again to reach a peak at $\alpha = 30\%$ (or $\tau \cong 5.4$ ms). The penetration then dropped off again at higher duty cycles. Similar observations

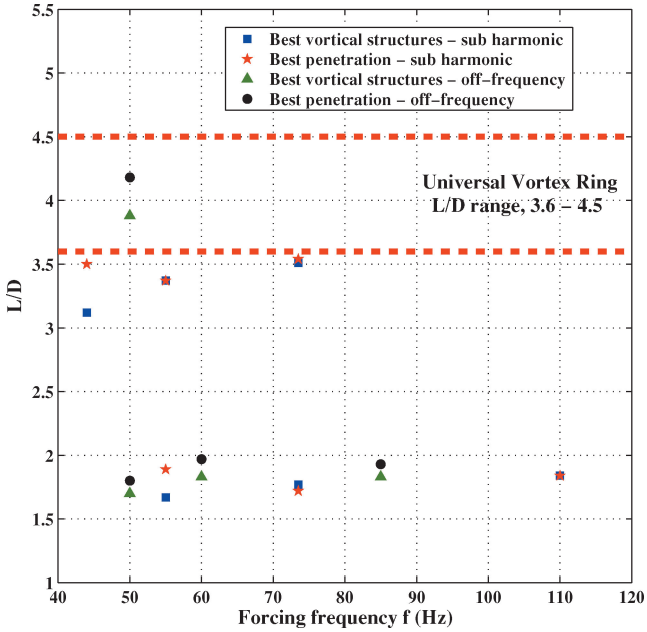

Fig. 7 Measured experimental *L/D* ratio for experimental case 1, with peak-to-peak ΔU_j = 4.8 m/s, as function of forcing frequency; universal timescale regime for *L/D* suggested by Gharib et al.[23] is shown for comparison.

of two optimal timescales were made for other forcing frequencies, whether subharmonic or nonsubharmonic.

Figure 7 shows a quantification of the observed optimal $L/D \equiv \Delta U_j \tau / D_j$ values, for example, as observed in the conditions with asterisks shown in Figs. 6a–6c for a wide range of excitation conditions. The observation of two distinct critical τ values resulted in two critical values of L/D, the first lying in the range 1.7–2.0 and the second in a range similar to that suggested by Gharib et al.,[23] 3.2–4.2. In some cases the conditions producing the clearest vortical structures are plotted, whereas in others those with the greatest vortex penetration are shown. The L/D ranges for these different optimally forced jets did not appear to depend significantly on either definition. Similarly, the L/D range did not appear to be sensitive to the forcing frequency (subharmonic of the fundamental vs a random forcing frequency). In fact, there was no obvious visual difference in jet behavior, for a fixed forcing frequency, between the two different critical L/D conditions. Yet clearly the timescales associated with the generic jet in crossflow should also influence time- and length scales leading to optimized formation of distinct vortical structures. This lower regime for L/D may reflect these transverse jet timescales. Exploration of the relation between the transverse jet's natural shear layer instabilities (especially in the

near field) and these additional timescales is the focus of ongoing research.[16–18]

Conclusions

The present experiments on the acoustically forced jet in crossflow suggested clear sets of excitation conditions that produced deeply penetrating jets, with corresponding formation of distinct, deeply penetrating vortical structures. When the rms of the velocity excitation was matched among different excitation conditions, single values of pulse width and a wide variety of frequencies (subharmonic as well as nonsubharmonic) were observed to generate deeply penetrating vortical structures and improved levels of jet penetration. As long as the forcing frequency was relatively low (in comparison to the upstream shear layer mode for the unforced transverse jet f_n), jet penetration and spread could be optimized through application of the appropriate pulse width τ_{opt}.

Note, however, that a maximum in jet penetration may not necessarily translate into an optimally mixed jet in crossflow because strongly bifurcated jets may have a lesser degree of quantified injectant mixedness than that of a jet with a more uniform spatial distribution of injectant. This suggests that acoustical forcing at very low relative frequencies, for example, as shown in Fig. 5b, may have benefits for enhanced mixing in that specific subharmonic frequencies are not required to achieve deep jet penetration. Thus, the duty cycle could be increased to produce a better-mixed jet in crossflow. The issue of optimal frequencies to achieve maximum jet penetration requires more extensive examination in the sense that large enough excitation velocities can force strong vortex roll up irrespective of the relation of the forcing frequency to the natural shear layer frequency.

The present experiments, at relatively low values of R (≤ 4), were generally consistent with the ideas of Gharib et al.[23] in terms of a critical stroke ratio associated with optimal vortex ring formation. Yet it is interesting to note that a second critical L/D ratio, roughly one-half of that predicted by Gharib et al. for vortex ring optimization, also produced deeply penetrating vortical structures and improved transverse jet penetration. One-half of an equivalent vortex ring stroke length would not fill the recirculation zone of a vortex ring, hence, it is interesting that these smaller L/D ratios produced such deeply penetrating vortical structures and jets. Timescales associated with the transverse jet (especially its upstream near-field shear layer) may well be coupled in such a way as to force vortex merger for these smaller L/D conditions.

Finally, it is of interest for these experiments at relatively low R that large-amplitude sinusoidal excitation did not produce any significant jet response when compared with the unforced jet in crossflow. Preliminary recent experiments[16,17] exploring differences in the transverse jet shear layer instability at high ($R > 5$) and low ($R < 5$) jet-to-crossflow velocity ratios suggest that optimal forcing conditions and transverse jet responses may in fact be dependent on the jet regime, that is, the value of R. Future study of the jet's response to forcing under a wide variety of transverse jet conditions, at low as well as high jet-to-crossflow velocity ratios, will elucidate these mechanisms.

Acknowledgments

The research reported here was supported by the National Science Foundation under Grant CTS-0200999 and by NASA Dryden Flight Research Center under Grant NCC4-153. The authors acknowledge the helpful assistance provided by University of California, Los Angeles, undergraduate student researchers Robert Lobbia, Lydia Trevino, Marcus George, Rebekah Tanimoto, and Andy Lutomirski and by recent graduate students Sevan Megerian and Juliett Davitian. The authors also acknowledge the extensive contributions made in the early stages of this study by Luca Cortelezzi of McGill University.

References

[1]Broadwell, J. E., and Breidenthal, R. E., "Structure and Mixing of a Transverse Jet in Incompressible Flow," *Journal of Fluid Mechanics*, Vol. 148, 1984, pp. 405–412.

[2]Fric, T. F., and Roshko, A., "Vortical Structure in the Wake of a Transverse Jet," *Journal of Fluid Mechanics*, Vol. 279, 1994, pp. 1–47.

[3]Kamotani, Y., and Greber, I., "Experiments on a Turbulent Jet in a Crossflow," *AIAA Journal*, Vol. 10, No. 11, 1972, pp. 1425–1429.

[4]Kelso, R. M., Lim, T. T., and Perry, A. E., "An Experimental Study of Round Jets in Cross-Flow," *Journal of Fluid Mechanics*, Vol. 306, 1996, pp. 111–144.

[5]Smith, S. H., and Mungal, M. G., "Mixing, Structure and Scaling of the Jet in Crossflow," *Journal of Fluid Mechanics*, Vol. 357, 1998, pp. 83–122.

[6]Cortelezzi, L., and Karagozian, A. R., "On the Formation of the Counter-Rotating Vortex Pair in Transverse Jets," *Journal of Fluid Mechanics*, Vol. 446, 2001, pp. 347–373.

[7]M'Closkey, R. T., King, J. M., Cortelezzi, L., and Karagozian, A. R., "The Actively Controlled Jet in Crossflow," *Journal of Fluid Mechanics*, Vol. 452, 2002, pp. 325–335.

[8]Vermeulen, P. J., Grabinski, P., and Ramesh, V., "Mixing of an Acoustically Excited Air Jet with a Confined Hot Crossflow," *Journal of Engineering for Gas Turbines and Power*, Vol. 114, 1992, pp. 46–54.

[9]Johari, H., Pacheco-Tougas, M., and Hermanson, J. C., "Penetration and Mixing of Fully Modulated Turbulent Jets in Crossflow," *AIAA Journal*, Vol. 37, No. 7, 1999, pp. 842–850.

[10]Eroglu, A., and Breidenthal, R. E., "Structure, Penetration, and Mixing of Pulsed Jets in Crossflow," *AIAA Journal*, Vol. 39, No. 3, 2001, pp. 417–423.

[11]Schuller, T., King, J., Majamaki, A., Karagozian, A. R., and Cortelezzi, L., "An Experimental Study of Acoustically Controlled Gas Jets in Crossflow," *Bulletin of the American Physical Society*, Vol. 44, No. 8, 1999, p. 111.

[12]Narayanan, S., Barooah, P., and Cohen, J. M., "Dynamics and Control of an Isolated Jet in Crossflow," *AIAA Journal*, Vol. 41, No. 12, 2003, pp. 2316–2330.

[13]Johari, H., "Scaling of Pulsed Jets in Crossflow," AIAA Paper 2005-304, Jan. 2005.

[14]Andreopoulous, J., "On the Structure of Jets in a Crossflow," *Journal of Fluid Mechanics*, Vol. 157, 1985, pp. 163–197.

[15]Moussa, Z. M., Trischka, J. W., and Eskinazi, S., "The Nearfield in the Mixing of a Round Jet with a Cross-stream," *Journal of Fluid Mechanics*, Vol. 80, 1977, pp. 49-80.

[16]Karagozian, A. R., Megerian, S., Alves, L., George, M., Kelly, R. E., and M'Closkey, R. T., "Control of Vorticity Generation in an Acoustically Excited Jet in Crossflow," AIAA Paper 2005-0303, Jan. 2005.

[17]Megerian, S., and Karagozian, A. R., "Evolution of Shear Layer Instabilities in the Transverse Jet," AIAA Paper 2005-0142, Jan. 2005.

[18]Alves, L. S. de B., Kelly, R. E., and Karagozian, A. R., "Linear Stability Analysis of Jets in Crossflow," AIAA Paper 2005-1118, Jan. 2005.

[19]King, J. M., "The Actively Controlled Jet in Crossflow," M.S. Thesis, Dept. of Mechanical and Aerospace Engineering, Univ. of California, Los Angeles, June 2002.

[20]Lobbia, R., Shapiro, S., M'Closkey, R. T., and Karagozian, A. R., "Feedback Compensation for Real-Time Control of Transverse Jet Injection," *Bulletin of American Physical Society*, Vol. 47, No. 8, 2002, p. 92.

[21]George, M. R., "Closed Loop Control of Transverse Jet Instabilities," M.S. Thesis, Dept. of Mechanical and Aerospace Engineering, Univ. of California, Los Angeles, June 2006.

[22]Ho, C.-M., and Huerre, P., "Perturbed Free Shear Layers," *Annual Review of Fluid Mechanics*, Vol. 16, 1984, pp. 365–424.

[23]Gharib, M., Rambod, E., and Shariff, K., "A Universal Time Scale for Vortex Ring Formation," *Journal of Fluid Mechanics*, Vol. 360, 1998, pp. 121–140.

N. Chokani
Associate Editor